Clin Orthop Relat Res (2026) 484:81-94
DOI 10.1097/CORR.0000000000003613

Clinical Orthopaedics and Related Research®
A Publication of The Association of Bone and Joint Surgeons®

Clinical Research

Fifth Metatarsal Stress Fractures Are Associated With Increased Bone Density and Altered Alignment on Weightbearing CT

François Lintz MD, PhD[1,2], Wolfram Grün MD[2,3,4], Enrico Pozzessere MD[2], Emily Luo BS[2], Erik Jesus Huanuco Casas MD[2,5], Pierre-Henri Vermorel MD[2,6], Antoine Acker MD[2,7], Cesar de Cesar Netto MD, PhD[2]

Received: 11 February 2025 / Accepted: 20 June 2025 / Published online: 10 July 2025

Abstract

Background Stress fractures of the fifth metatarsal (M5) are common among individuals engaging in repetitive impact activities or patients with preexisting deformities. Compared with patients who have traumatic fractures, those with stress fractures often develop delayed union, nonunions, or recurrence. Risk factors such as hindfoot varus and foot adduction have been implicated. The recent advent of weightbearing CT enables the study of specific bone density and orientation characteristics that have not, to our knowledge, previously been explored. Such tools could detect higher risk patients and help trigger potential preventive measures.

Questions/purposes Do patients with an M5 stress fracture present altered three-dimensional orientation and alignment parameters compared with an age- and sex-matched control group? (2) Do the feet and M5s of patients with an M5 stress fracture present different foot ankle offset (FAO) parameters compared with the control group? (3) Do the M5s of patients with an M5 stress fracture present with altered bone density patterns compared with

One of the authors (FL) certifies receipt of personal payments or benefits, during the study period, in an amount of less than USD 10,000 from Paragon 28 and in an amount of less than USD 10,000 from CurveBeam AI. One of the authors (CDCN) certifies receipt of personal payments or benefits, during the study period, in an amount of less than USD 10,000 from Paragon 28.
Clinical Orthopaedics and Related Research® neither advocates nor endorses the use of any treatment, drug, or device. Readers are encouraged to always seek additional information, including FDA approval status, of any drug or device before clinical use.
Ethical approval for this study was obtained from the DUHS Institutional Review Board (Protocol ID: Pro00113556, Reference ID: Pro00113556-INIT-1.0).
The work was performed at the Division of Foot and Ankle Surgery, Department of Orthopaedic Surgery, Duke University School of Medicine, Durham, NC, USA.

[1]Ramsay Healthcare, Clinique de l'Union, Department of Foot and Ankle Surgery, Saint Jean, France

[2]Department of Foot and Ankle Surgery, Department of Orthopaedic Surgery, Duke University School of Medicine, Durham, NC, USA

[3]Department of Orthopaedic Surgery, Østfold Hospital Trust, Grålum, Norway

[4]Institute of Clinical Medicine, University of Oslo, Oslo, Norway

[5]Clínica Delgado Auna - Auna Perú, Lima, Peru

[6]Saint Etienne University Hospital, Saint Etienne, France

[7]Centre of Foot and Ankle Surgery, Clinique La Colline, Geneva, Switzerland

F. Lintz ✉, Ramsay Healthcare, Clinique de l'Union, Department of Foot and Ankle Surgery, 31240, Saint Jean, France, Email: francois.lintz@duke.edu

Wolters Kluwer

the control group, and is a clinically relevant threshold identifiable?

Methods This institutional review board–approved retrospective case-control study analyzed 15 feet of patients with M5 stress fractures and 15 feet of a control group using weightbearing CT. Between February 2022 and May 2024, a total of 74 patients with available weightbearing CT scans were treated for an M5 fracture. Among those patients, we considered 77% (57) of proximal fractures as potentially eligible. Of those patients, 39% (22 of 57) were included; a further 32% (7 of 22) were later excluded because of metal artifact conflicting with M5 bone density assessment, leaving 68% (15 of 22) for analysis here. Controls were selected from our weightbearing CT archive, matched for age and sex and excluded if any foot disorder or prior intervention was identified. Accordingly, there were seven males and eight females in each group, and five and nine left sides, respectively, in the stress fractures and control groups. The mean ± SD age was 53 ± 13 years for the stress fractures group versus 51 ± 12 years for controls. Mean ± SD BMI was 34.4 ± 10.2 kg/m^2 for the stress fractures group and 36.8 ± 8.2 kg/m^2 for controls. For the first study question, M5 orientations and baseline foot alignment parameters were evaluated based on Digital Imaging and Communications in Medicine (DICOM) data sets using weightbearing CT software. For the second study question, weightbearing CT software was used to measure the FAO and assess the spatial relationship of the M5 with the foot tripod. For the third study question, segmentation and bone density measurements, using Hounsfield units (HUs), were performed with commercially available and open-source software. Receiver operating characteristic analysis with the Youden index was performed to determine the sensitivity and specificity of the HU M5/HU talus density ratio for identifying stress fractures.

Results The stress fractures group exhibited a lower M5 base height at mean ± SD 9 ± 3 mm versus 12 ± 3 mm ($p = 0.045$), greater ground contact frequency (11 of 15 versus 0 of 15 for the control group; $p < 0.001$), and an increased median (range) M5/M4 length ratio of 1.06 (0.95 to 1.14) versus 1.01 (0.97 to 1.10) for controls ($p = 0.04$). Hindfoot varus and foot adduction were associated with stress fractures, as indicated by altered hindfoot alignment and tarsometatarsal angles. The stress fractures group demonstrated a mean 50% increase in the HU M5/HU talus density ratio, at a median (range) of 1.52 (0.9 to 2.3) versus 1.02 (0.97 to 1.1) ($p < 0.001$). A relative increase by a factor of 1.2 in the HU M5/HU talus density ratio was associated with the stress fractures group with 80% sensitivity and 94% specificity.

Conclusion Stress fractures of the M5 are known to be associated with hindfoot varus and forefoot adductus. The present study adds that these injuries may also be associated with reduced base height, increased plantarflexion, a longer M5, and higher bone density. Future prospective studies could investigate whether using a threshold of 1.2 for the HU M5/HU talus density ratio to trigger early preventive measures could help decrease the occurrence of stress fractures.

Level of Evidence Level III, prognostic study.

Introduction

Stress fractures are a common condition affecting individuals subject to deformities or repetitive impact activities, where the natural repair cycle of bones is overwhelmed [10, 14, 22]. The foot is one of the most common locations, representing up to 50% of occurrences of stress fractures [14]. Frequency has been reported at 5.7 per 100,000 accident exposures in a database study of over 10 million college athlete exposures [28]. The metatarsals represent the most frequent site in the foot at 37.9%, in particular, the second, third, and fifth metatarsals [1], but stress fractures may also affect other bones such as the calcaneus, navicular, or talus. Several activity-related or patient-specific factors [21, 32] are known to increase the risk of stress fractures: female sex, osteoporosis, metatarsus adductus [33], forefoot or hindfoot varus, neurovascular disorders [24], pronation [11], decreased dorsiflexion, a high arch [14], increased BMI, altered vitamin D metabolism [23, 29], and muscular fatigue [9].

Some stress fractures have been referred to as "high risk" [4, 6, 29]. Among these, the fifth metatarsal (M5) is the most frequent location [4, 6, 12, 29] and corresponds to Zone 3 or the metaphyseal zone in the anatomic Lawrence and Botte [15] classification, where Zones 1 through 3 are described from proximal to distal and Type 1 and Type 2 concern the proximal epiphysis. Other classifications such as that of Torg et al. [34], based on the radiologic description of the fracture line characteristics from fresh (Type 1) to sclerotic (Type 3), do not account for differences in pathogenesis. In practice, the historical "Jones" eponym [13], historically described as a metaphyseal-diaphyseal junction fracture, is commonly indifferently used for proximal M5 fractures, which has also led to confusion and inconsistencies as to the appropriate evaluation of Zone 3 stress fractures. Local conditions such as tensile load or poor vascularity [30] are thought to result in increased risk for delayed union, nonunion, or progression to complete fracture, but the biomechanical and physiologic rationale behind these changes remains poorly understood and constitutes a knowledge gap [2]. In particular, specific M5 spatial orientation and bone density parameters remain unknown. In the past, imaging modalities (two-dimensional [2D] radiography and nonweightbearing CT) limited the ability to capture these potentially informative data. The advent of weightbearing CT offers new perspectives as it offers low-dose, in-office three-

dimensional (3D) weightbearing imaging that has demonstrated improved risk assessment in ankle instability [17], osteoarthritis [19], and malalignment [18, 26] by quantifying 3D alignment and bone density topography [18]. Advances in semiautomatic [20, 37] and automated tools [5] have enhanced diagnostic speed [27] and clinical relevance [7] and may help elucidate stress fracture mechanisms.

We therefore asked: (1) Do patients with an M5 stress fracture present altered 3D orientation and alignment parameters compared with an age- and sex-matched control group? (2) Do the feet and M5s of patients with an M5 stress fracture present different foot ankle offset (FAO) parameters compared with the control group? (3) Do the M5s of patients with an M5 stress fracture present with altered bone density patterns compared with the control group, and is a clinically relevant threshold identifiable?

Patients and Methods

Overview of Study Design

In this retrospective comparative study, we analyzed existing data recorded as part of routine clinical care at our institution, a major academic institution in an urban area, within an orthopaedics and trauma department.

Study Population

We considered all adult patients (18 years or older) who underwent a weightbearing CT in our institution as part of the standard follow-up between February 2022 and May 2024 (using a PedCat/Hi-Rise® system [CurveBeam AI] with a voxel size of 0.37 mm, field of view diameter of 350 mm, field of view height of 200 mm, exposure time of 9 seconds, total scan time of 54 seconds, and monthly phantom calibration as per manufacturer and institutional protocols). Between February 2022 and May 2024, a total of 74 patients with available weightbearing CT scans were treated for an M5 fracture. Among those patients, we considered 77% (57) of proximal fractures as potentially eligible. Of those patients, 39% (22 of 57) were included; a further 32% (7 of 22) were later excluded because of metal artifact conflicting with M5 bone density assessment, leaving 68% (15 of 22) for analysis here (Fig. 1). All patients had a confirmed diagnosis of Zone 3 M5 stress fracture as assessed twice by two senior fellowship-trained orthopaedic foot and ankle surgeons (FL, WG). Diagnosis was established based on clinical history, examination, and weightbearing CT findings. Exclusion criteria were patients younger than 18 years; any previous disorder (neuropathy), trauma, or surgery (such as osteotomy, arthroplasty, or fusion) that could affect foot ankle alignment; and no weightbearing CT results available before surgical treatment of M5 fracture, as the presence of metal would have hindered the bone density analysis. Medical records were retrieved, and we extracted a sample of 15 feet from 14 patients per study inclusion and exclusion criteria.

A control group was included using 15 asymptomatic feet with clinically normal alignment as assessed by a trained clinician (WG) from 15 individuals without history of surgery affecting alignment or treatment affecting bone density. Controls were the contralateral sides from patients who were consulting for another unilateral disorder with available bilateral weightbearing CT results. Demographics were recorded, including age, side, sex, and BMI. The groups were matched by pairs for age and sex, which are known to influence bone density [28, 31, 35].

Demographic Data

There were seven males and eight females in each group, and five and nine left sides, respectively, in the stress fractures and control groups. Side and sex distributions were not different between the two groups. The mean ± SD age was 53 ± 13 years for the stress fractures group versus 51 ± 12 years for the control group ($p = 0.97$). Mean ± SD BMI was 34.4 ± 10.2 kg/m^2 for the stress fractures group and 36.8 ± 8.2 kg/m^2 for the control group ($p = 0.50$) (Table 1).

Primary, Secondary, and Tertiary Study Outcomes

The primary outcome measure was the Hounsfield unit (HU) M5/HU talus density ratio. The secondary outcomes were as follows: forefoot arch angle; M5 base height; Meary (talus-M1) axial and sagittal angles; calcaneus inclination angle; Saltzman Hindfoot alignment angle; hindfoot moment arm; first, second, and third tarsometatarsal axial and sagittal angles; M4-M5 axial and sagittal (inclination) angles; talus-to-M5 axial and sagittal (inclination) angles; M5-to-fifth-toe axial angle; M5 centroid height; M5-to-M4 volume ratio; M5-to-M4 length ratio; and M5-to-M4 HU ratio. The tertiary outcomes were FAO and modified FAO values and visual assessment, including whether the M5 base or head was in closer contact with the ground plane (M5 inclination) and the relationship of the talus point with the lateral border of the foot (inside or outside the tripod).

Image Processing and Measurements

Presegmentation Steps

The following measurements were performed manually: forefoot arch angle as previously described [8] (coronal angle

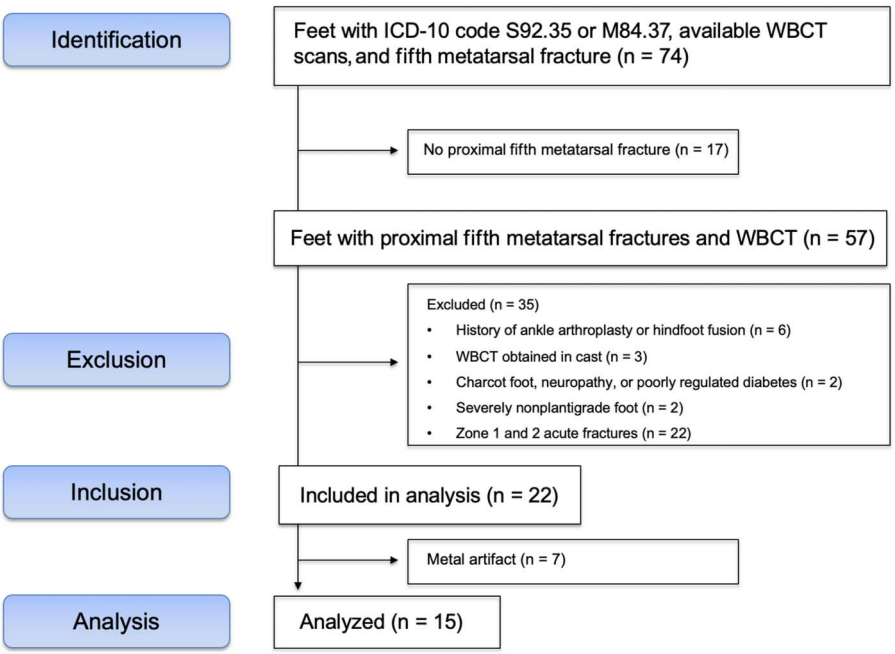

Fig. 1 Flow chart representing patient selection. WBCT = weightbearing CT.

between the ground and the line joining the most proximal, plantar point of the medial cuneiform and the most plantar point of the M5 base) and M5 base height from the ground plane (Fig. 2). We used the Digital Imaging and Communications in Medicine (DICOM) data sets with the available Cubevue® 3D viewer (CurveBeam AI) and the viewer's native standard measurements tool (distances, angles). To visually assess M5 inclination, we recorded whether the base or the head of the M5 was seen first as the distal axial slice was brought more proximal in the visualizer (Fig. 3). M5 base measurements were then taken in the sagittal plane (Fig. 4A-B). Two observers, both senior fellowship-trained foot and ankle surgeons (FL, WG), performed these measurements to assess for interobserver reliability. The first investigator (FL) performed the measurements again after a 1-month washout period to assess intraobserver reliability.

Regarding semiautomatic measurements, we measured hindfoot alignment using the FAO via the TALAS® tool in Cubevue as previously described [20], including the previously published normative data; this allowed us to check that the control group was correctly aligned. Given that in some cases the M5 base would touch the ground plane before the head (decreased M5 slope), we calculated the FAO twice (FAO and modified FAO configurations) using the head or the base as the M5 point to define the foot tripod and its position relative to the center of the ankle. A similar methodology was described recently by Bernasconi et al. [3] in cavovarus feet for the calcaneal point of the tripod. Furthermore, we recorded in both configurations (FAO and modified FAO) whether the point representing the talus, or center of the ankle, was projected within or outside of the foot tripod. This corresponded to the weightbearing center

Table 1. Group descriptive statistics and comparability

Patient characteristic	Stress fractures group (n = 15)	Control group (n = 15)	p value
Sex			> 0.99
Male	7	7	
Female	8	8	
Age in years	53 ± 13	51 ± 12	0.97
Side			0.27
Left	5	9	
Right	10	6	
BMI in kg/m^2	34.4 ± 10.2	36.8 ± 8.2	0.50

Data presented as the number or mean ± SD.

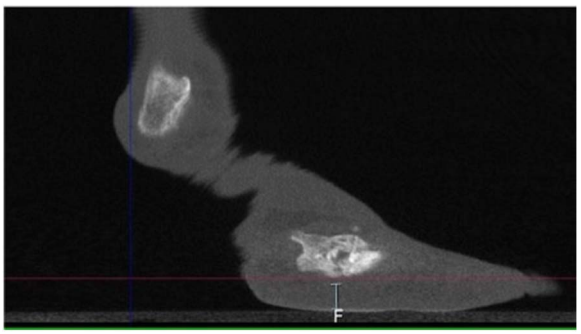

Fig. 2 The figure presents a typical measurement from the ground plane up to the lowest point on the M5 base. The vertical line ("Floor" [F]) represents the measurement tool, which is extended to the red line. The red line represents the axial plane being scrolled up to the level of the first pixel belonging to the M5 base.

of the ankle projecting vertically lateral (outside) or medial (inside) relative to the lateral border of the foot tripod. The foot tripod was defined through selection of the M1, M5, and calcaneus weightbearing points (Fig. 5) and represented in the output window of the TALAS tool (Fig. 6A-B).

Segmentation

Each foot data set was semiautomatically segmented using BoneLogic® Disior™ (Paragon 28), a commercial

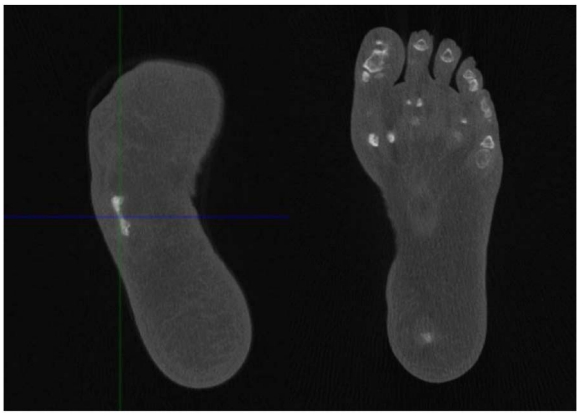

Fig. 3 On the left (right foot, stress fractures group), the axial slice containing the lowest points on the M5 is shown. On the right (left foot, control group), the tripod appears balanced, with simultaneous visualization of the M1, M5, and the calcaneus as the axial slice is scrolled up. To ensure that visualization of the tripod was not sensitive to orientation, the horizontal slice, coplanar with the ground, was systematically used and scrolled vertically.

Fig. 4 (**A**) An image from the control group showing a 5-mm-wide sagittal slice including the M5 where the base is higher than the head. (**B**) An image from the stress fractures group showing remodeled bone following an M5 stress fracture on the same slice, where the base is lower than the head. Blue vertical lines represent the highest distance from the floor (F, red horizontal line). Red vertical lines represent the shortest distance from F. Of note, the presence of a substantial amount of remodeled bone dorsally means that the mechanical axis will not necessarily horizontalize because it considers bone density; this is why inclination measurements were also taken relative to the talus, not only relative to the M4. A color image accompanies the online version of this article.

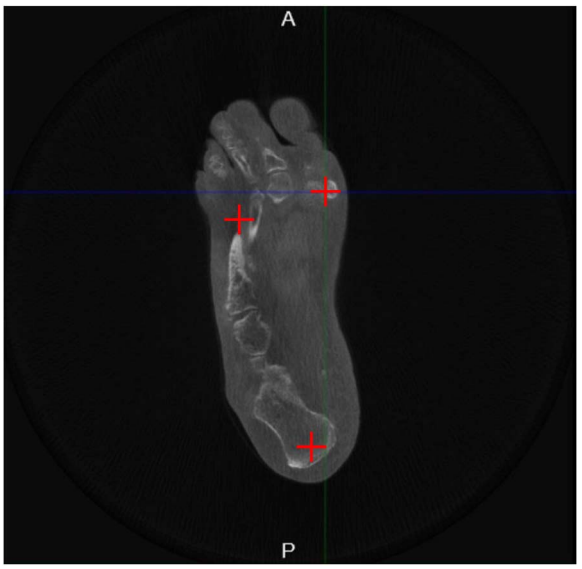

Fig. 5 Selection of the three tripod points for the foot ankle offset as originally described using the M5 head. A = anterior; P = posterior.

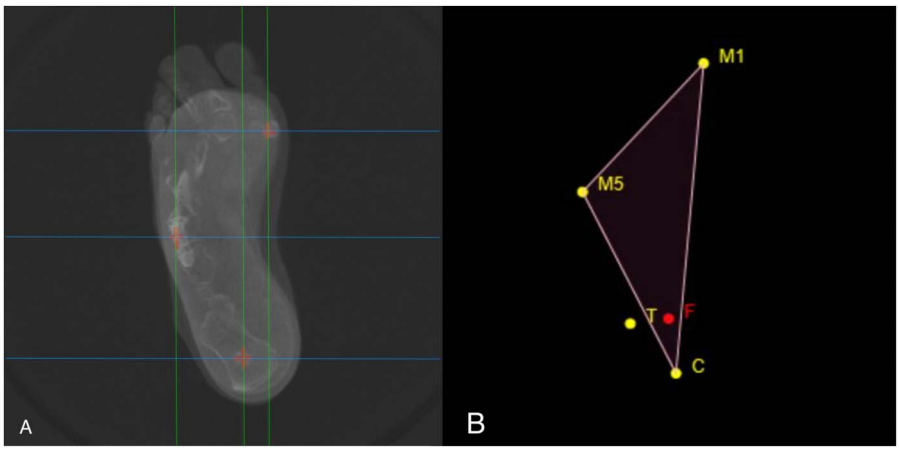

Fig. 6 (**A**) This figure results from superimposition of three axial planes including the M1 and M5 and calcaneus lowest points. The selection of the three tripod points for the foot ankle offset using the lowest point on the M5 base instead of the head is presented. The selection is made where the sagittal plane (green lines) and the coronal plane (blue lines) intersect. This measurement was also performed when the former was found to be lower than the latter. (**B**) Correspondence between the selection input and the measurement output in the window of the TALAS tool. The "T" point corresponds to the vertical projection of the center of the ankle. A "T" point falling outside of the tripod is indicative of a considerably imbalanced foot and ankle complex. The tripod is defined by the lowest point on the M1 head, the M5 head, and the calcaneus (C). The "TF" segment represents the FAO.

software available at our institution and previously described [18] (Fig. 7). Segmentations included the talus, M4, M5, and the fifth toe proximal phalanx; these were subsequently converted to 3D stereolithography (*.stl) files. To start, the process required labeling each bone manually. The software algorithm then proceeded with outlining each bone in 3D space based on density thresholding and identification of specific landmarks and interbone relationships. Once each bone was identified in each slice, the slices were stacked up together and the individual bones reconstructed. A segmentation report was finally retrieved with automatic extraction of the following conventional metrics, as previously described [25, 36]. Hindfoot metrics were as follows: Meary sagittal angle, calcaneal inclination sagittal angle, Saltzman tibiocalcaneal angle with 20° projection, hindfoot moment arm, and Meary axial angle (Fig. 8). Midfoot metrics were as follows: first tarsometatarsal axial and sagittal, second tarsometatarsal axial and sagittal, and third tarsometatarsal axial and sagittal angles.

Fig. 7 Illustrations of segmentation steps. (**A**) 3D rendering view showing manual labeling of the individual bones of interest (depending on study specifics); each selection of a bone for labeling results in visual marking by a colored dot. (**B**) 3D bone model showing rendering of full 3D models for visual inspection. (**C**) 3D measurements report showing acquisition of automated angular, distance, volumetric, and HU reports built from 3D analyses of relative and absolute bone axes, scalar data, and surface map coordinates. The report was exported to *xlsx.

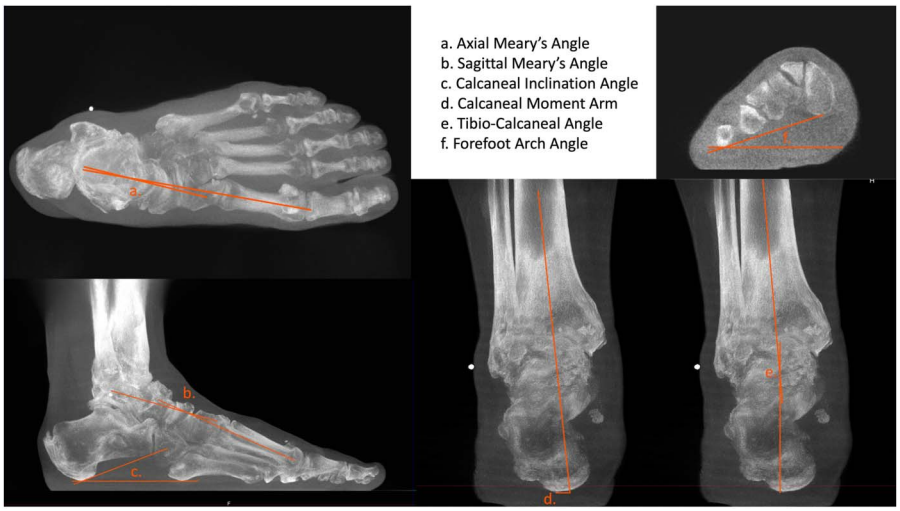

Fig. 8 Presentation of the six manual measurements performed in stress fractures and controls: (**a**) axial Meary angle, (**b**) sagittal Meary angle, (**c**) calcaneal inclination angle, (**d**) calcaneal moment arm, (**e**) tibiocalcaneal angle, and (**f**) forefoot arch angle.

Postsegmentation Steps

The following measurements were performed for the talus, M4, M5, and fifth toe proximal phalanx: HU-weighted centroid and longitudinal principal component axes coordinates, volume, length (for M4 and M5), and mean ± SD of HU values. All postsegmentation measurements were performed with the DICOM data sets and *.stl files loaded in 3D Slicer software, version 5.6.2 (open source, by Slicer Community) using the Label Map plugin of the Segment Statistics Module (Fig. 9). From these, we derived values for the M4-M5 and talus-M5 axial and sagittal angles (Fig. 10A-B), as well as for the M5–fifth toe proximal phalanx axial angle, the height of the M5 centroid (or HU-weighted center of mass), the length and volume ratios of M5/M4, and the HU M5/HU talus density ratio. The HU values given natively as voxel brightness were used as a proxy to bone density after normalization. Normalization was performed by obtaining an HU M5/HU talus density ratio. Indeed, as previously described [18], standalone HU values in CT are not recommended to evaluate bone density in the absence of a normalization using a hydroxyapatite phantom for each scan as they are too variable. According to good practice in that case, the mean HU of any single bone (in this case, the talus) serves as an internal phantom. Therefore, we normalized M5 HU values relative to talus HU values.

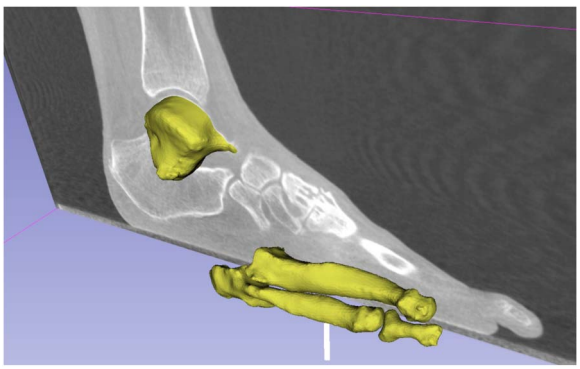

Fig. 9 This is an illustration of stereolithographic models (*.stl files) for the talus, M5 and M4, and the fifth toe proximal phalanx that were loaded in the DICOM volume via 3D Slicer software. Absolute and relative 3D orientations were recorded, and density values were normalized relative to the density of the talus. A color image accompanies the online version of this article.

Ethical Approval

Ethical approval for this study was obtained from the DUHS Institutional Review Board (Protocol ID: Pro00113556, Reference ID: Pro00113556-INIT-1.0).

Statistical Analysis

Normality and heteroskedasticity of continuous data were assessed with the Shapiro-Wilk and Levene tests, respectively. Continuous variables were expressed as mean ± SD and discrete outcomes as absolute frequencies and range. We assessed group comparability by comparing baseline demographic data between groups. Considering our small sample size, equal representation of males and

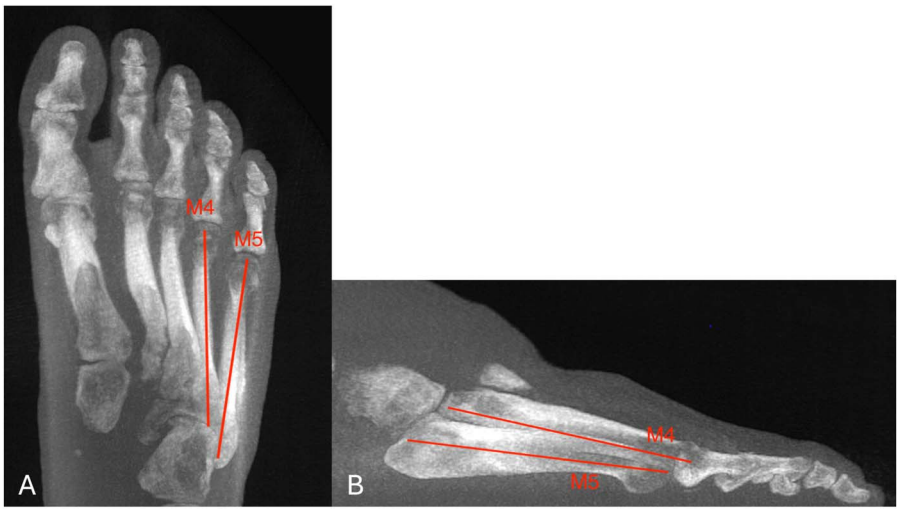

Fig. 10 (**A**) An example of the axial M4-M5 angle measurement demonstrating the relative plantarflexion angle of M5 relative to M4. (**B**) An example of the sagittal M4-M5 angle measurement demonstrating the relative abduction angle of M5 relative to M4.

females could not be ensured, and no by-sex disaggregation of data or analysis was conducted. Continuous outcomes were compared using an unpaired Student t-test, Welch t-test, or Mann-Whitney U test according to data distribution. Discrete outcomes were compared with the chi-square or the Fisher exact test, accordingly. The significance level was set to 5%, and we used two-tailed tests. Intraclass correlation coefficients (ICC) estimates and their 95% confidence intervals (CIs) were calculated to assess interobserver reliability of manual measurements. ICC values < 0.5, between 0.5 and 0.75, between 0.75 and 0.9, and > 0.9 were considered as poor, moderate, good, and excellent reliability, respectively. Absolute percentages of agreement and unweighted Cohen kappa values were used for discrete variables. We used receiver operating characteristic (ROC) curves and resulting area under the curve (AUC) for sensitivity and specificity of a stress fracture based on the HU M5/HU talus density ratio. The AUC, 95% CIs, and the Youden optimal threshold were calculated. Statistical analysis was performed with EasyMedStat, version 3.37.1 (EasyMedStat).

Interobserver and Intraobserver Agreement

For semiautomatic modified hindfoot alignment considering the M5 base as a weightbearing point for the foot tripod (reviewer 1 modified FAO versus reviewer 2 modified FAO), there was good interobserver agreement, with an ICC of 0.86 (95% CI 0.72 to 0.93; $p < 0.001$). The mean ± SD difference between the two observers was 1.6 ± 3.21 (95% CI 0.42 to 2.77). For M5 base height (reviewer 1 M5 base height versus reviewer 2 M5 base height), there was moderate interobserver agreement, with an ICC of 0.7 (95% CI 0.43 to 0.84; $p < 0.001$). The difference between the two observers was -1.34 ± 2.22 (95% CI -2.15 to -0.522). The assessment of whether the M5 base touched the ground plane first demonstrated almost perfect interobserver agreement, with an absolute agreement in 14 of 15 cases ($\kappa = 0.86$ [95% CI 0.66 to 1.05]). Regarding the projection of the center of the ankle point within or outside the FAO tripod, moderate overall agreement was found, with observers agreeing in 12 cases ($\kappa = 0.59$ [95% CI 0.35 to 0.83]) when the M5 base was considered as the weightbearing point, and substantial agreement, with observers agreeing in 13 cases ($\kappa = 0.73$ [95% CI 0.51 to 0.96]) when the M5 head was considered. Intraobserver agreement for the modified FAO and M5 height was excellent for both (Table 2). Intraobserver agreement was perfect for visual assessment of M5 inclination and FAO projection (absolute agreement in 15 of 15 cases for both).

Results

3D Orientation

Manual Measurements

The stress fractures group had an M5 base more plantar than controls (mean ± SD 9 ± 3 mm versus 12 ± 3 mm, mean difference -2 [95% CI -5 to 0]; $p = 0.045$) and no difference in forefoot arch angle (20° ± 12° versus 14° ± 5°; $p = 0.29$).

Table 2. FAO and M5 base height intraobserver reproducibility

Variable	Absolute agreement	ICC (95% CI)	p value
Modified FAO	14 of 15	0.94 (0.88-0.97)	< 0.001
M5 base height	15 of 15	0.76 (0.61-0.87)	< 0.001

Semiautomatic Measurements

The stress fractures group had an increased axial Meary angle (-5° ± 15° versus 9° ± 6°, mean difference -15° [95% CI -23° to -6°]; p < 0.01), second (4° ± 5° versus 8° ± 2°, mean difference -3° [95% CI -6° to 0°]; p = 0.03) and third (-10° ± 7° versus -5° ± 3°, mean difference -5° [95% CI -9° to -2°]; p = 0.01) tarsometatarsal sagittal angles, and increased first (median [range] -29° [-39° to -22°] versus -23° [-30° to -13°], difference of medians -4°; p = 0.002), second (-29° ± 5° versus -20° ± 4°, mean difference -9° [95% CI -12° to -6°]; p < 0.001), and third (-27° ± 7° versus -20° ± 4°, mean difference -7° [95% CI -11° to -3°]; p = 0.002) tarsometatarsal axial angles (Table 3). The stress fractures group had decreased (more varus) hindfoot moment arm (-2 ± 11 mm versus 5 ± 6 mm, mean difference -8 mm [95% CI -14 to -2]; p = 0.02) and more varus Saltzman angles (18° ± 13° versus 7° ± 10°, mean difference 11° [95% CI 3° to 20°]; p = 0.02). No differences were found in Meary sagittal (-8° ± 14° versus -8° ± 5°; p = 0.89), calcaneal inclination (median [range] 17° [8° to 25°] versus 21° [9° to 31°]; p = 0.21), and first tarsometatarsal sagittal (7° ± 4° versus 9° ± 1°; p = 0.07) angles compared with controls.

Postsegmentation Measurements

The stress fractures group presented an increase in axial (20° ± 8° versus 32° ± 7°, mean difference -12° [95% CI -17° to -6°]; p < 0.001) and sagittal (17° ± 9° versus 11° ± 6°, mean difference 6° [95% CI 1° to 11°]; p = 0.04) talus-M5 angles and an increased M5/M4 length ratio (median [range] 1.06 [0.95 to 1.14] versus 1.02 [0.97 to 1.10], difference of medians 0.06; p = 0.04) compared with controls (Table 4).

FAO Parameters

The stress fractures group had decreased (more varus) FAO (-5° ± 8° versus 2° ± 3°, mean difference -6° [95% CI -11° to -2°]; p = 0.01), with the talus point more frequently projecting outside the foot tripod (15 of 15 versus 10 of 15; p = 0.04), and inverse M5 inclination (the M5 base was lower than the head), with the M5 base touching the ground plane first in 11 of 15 cases for the stress fractures group versus 0 of 15 for controls (p < 0.001) (Table 3). Considering the modified FAO tripod, no difference was found in modified FAO (median [range] -1° [-17° to 4°] versus 1° [-5° to 8°]; p = 0.07) or talus point projection for the stress fractures group compared with controls (the talus point was in the tripod in 13 of 15 cases in both groups; p > 0.999).

Bone Density Patterns and Threshold Ratio

No difference in talus HUs was found between the two groups (mean ± SD 493 ± 171 for the stress fractures

Table 3. Semiautomatic measurements

Measurement	Stress fractures group	Control group	p value
Hindfoot alignment (FAO) in %	-4.5 ± 8.1 (-9.0 to 0.0)	1.5 ± 2.6 (0.1 to 3.0)	0.01
Saltzman angle	18 ± 13 (11 to 25)	7 ± 10 (1 to 13)	0.02
Posterior hindfoot moment arm in mm	-2 ± 11 (-8 to 3)	5 ± 6 (2 to 9)	0.02
Sagittal Meary (talus-M1) angle	-8 ± 14 (-16 to 0)	-8 ± 5 (-11 to -6)	0.89
Calcaneal inclination angle	17 (8 to 25)	21 (9 to 31)	0.21
Second tarsometatarsal sagittal angle	4 ± 5 (2 to 7)	8 ± 2 (7 to 8)	0.03
Third tarsometatarsal sagittal angle	-10 ± 7 (-13 to -6)	-5 ± 3 (-6 to -3)	0.01
Axial Meary angle	-5 ± 15 (-14 to 3)	9 ± 6 (6 to 13)	0.002
First tarsometatarsal axial angle	-29 (-39 to -22)	-23 (-30 to -13)	0.002
Second tarsometatarsal axial angle	-29 ± 5 (-31 to -26)	-20 ± 4 (-22 to -18)	< 0.001
Third tarsometatarsal axial angle	-27 ± 7 (-31 to -24)	-20 ± 4 (-25 to -18)	0.002

Data presented as mean ± SD (95% CI) or median (range). All angular measurements are in degrees.

Table 4. Postsegmentation measurements

Measurement	Stress fractures group	Control group	p value
Relative HU (M5/talus ratio)	1.52 (0.9-2.3)	1.01 (0.97-1.1)	< 0.001
Axial alignment of M5	20 ± 8 (15-25)	32 ± 7 (28-35)	< 0.001
Sagittal alignment of M5	17 ± 9 (12-21)	11 ± 6 (8-14)	0.04
M5 relative axial alignment to M4	7 ± 3 (5-8)	5 ± 1 (3-9)	0.07
M5 relative sagittal alignment to M4	8 ± 4 (6-10)	7 ± 2 (5-6)	0.19
Fifth toe adduction	8 (1-15)	21 (1-43)	0.25
M5 centroid height in mm[a]	21 ± 2 (20-23)	23 ± 3 (22-25)	0.09
Volume ratio of M5 to M4	1.21 ± 0.20 (1.10-1.33)	1.11 ± 0.08 (1.07-1.15)	0.09
Length ratio of M5 to M4	1.06 (0.95-1.14)	1.02 (0.97-1.10)	0.04
Talus HU	393 ± 147 (312-475)	494 ± 171 (399-589)	0.10

Data presented as median (range) or mean ± SD (95% CI). All angular measurements are in degrees.
[a]The centroid is the center of mass of the M5.

group versus 393 ± 146 for controls; p = 0.10). Patients in the stress fractures group demonstrated higher HU M5/HU talus density ratios than did individuals in the control group (median [range] 1.52 [0.9 to 2.3] versus 1.01 [0.97 to 1.1], difference of medians 0.42; p = 0.001) (Table 4). The Youden optimal threshold was 1.2 for the HU M5/HU talus density ratio to identify higher risk of stress fractures, with an AUC of 0.87 (95% CI 0.74 to 1), sensitivity of 80% (95% CI 0.57 to 1.00), specificity of 93.9% (95% CI 0.78 to 1.00), positive predictive value of 92.3% (95% CI 0.75 to 1.00), and negative predictive value of 82.4% (95% CI 0.60 to 1.00) (Fig. 11).

Discussion

Stress fractures, especially of the M5, are common in individuals involved in repetitive impact activities and in those with anatomic or physiologic risk factors. Conventional imaging modalities have limitations in capturing 3D alignment and bone density topography, which is essential for understanding these stress fractures. This study utilized 3D weightbearing CT imaging to investigate previously unclear bone density and local anatomic alignment characteristics associated with M5 stress fractures. To the best of our knowledge, the

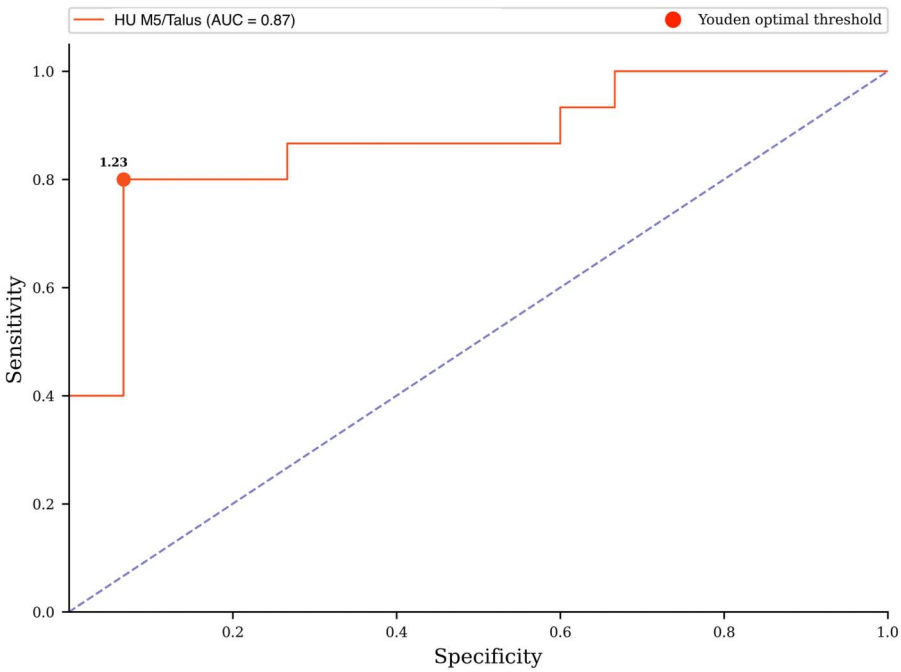

Fig. 11 The ROC curve with Youden optimal threshold and AUC of stress fractures relative to the HU M5/HU talus density ratio.

present study is the first to use advanced 3D weightbearing CT assessment for investigation of specific M5 parameters, particularly bone density, that are associated with stress fractures. Patients with M5 stress fractures demonstrated elevated localized bone density and altered 3D orientation, including increased varus hindfoot alignment, compared with matched controls. Accurate identification and understanding of these risk factors are essential for patient care and prevention strategies. Weightbearing CT imaging may thus enhance clinical assessment, allowing clinicians to better identify at-risk individuals, refine diagnosis, and potentially improve preventive care.

Limitations

We acknowledge several limitations in the present study. First, we had a small study population, which may theoretically have limited the generalizability of our findings; however, the population was large enough to identify between-group differences. Some differences might have been missed because of insufficient sample size, but those did not concern our key, clinically relevant findings and therefore would not have changed our conclusions. Also, the M5 metaphyseal stress fracture studied here is typical in its presentation, so a small sample is likely representative of a larger population. We did not intentionally select patients based on predefined radiographic or clinical criteria. The cohort represents a convenience sample, reflecting routine clinical presentation, but we believe that the way we arrived at our study group did not introduce selection bias.

Second, regarding repeatability of measurements, we only involved two observers to assess measurement reproducibility. However, we observed excellent absolute agreements and kappa values for the easily accessible visual, semiautomatic assessments. Additionally, our calculated density ratio is automatic and therefore does not involve human observers. Therefore, we feel that our conclusions were not affected by our choice of observers.

Third, weightbearing CT is not available in all centers, potentially limiting the current clinical impact of our study. Nonetheless, it is seeing wider use, and our study offers some values that could be helpful to centers that have (or soon will have) this clinical tool. Also, some patients who might not have benefited from weightbearing CT at the time of diagnosis may have been referred at a different stage of treatment, leading to differences in weightbearing that could affect bone density or alignment metrics. To account for this and avoid cotreatment bias, we excluded patients who were wearing a cast at the time of the scan.

Fourth, bone density is multifactorial; as such, beyond our findings, increased activity in the population at higher risk of stress fractures or abnormal kinematics such as lateral overload or stiffness may also have partly contributed to the occurrence of stress fractures. However, as these factors are not independent from bone density, this does not impact the relevance of our findings, but rather warrants a personalized approach for each patient. Finally, the absence of a by-sex analysis because of the lack of statistical power limited our ability to detect differences across sexes. Nevertheless, although alignment parameters and absolute bone density may indeed vary by sex, our primary outcome employed a normalized density ratio, which limits the impact on the interpretation of our results.

Discussion of Key Findings

In this study of patients presenting with stress fractures of the M5, we found altered 3D orientation, including a base closer to the ground plane, increased adduction, and declination relative to the talus. We found that in these patients, hindfoot varus and foot adduction was increased, confirming previous findings [11, 14, 33]. Furthermore, according to our data, for each 1° increase in hindfoot varus, M5 plantarflexion increased by 15%. Interestingly, we also found that the M5 was relatively longer compared with the M4 in the stress fractures group. Among previous studies on M5 fractures, few specifically addressed Zone 3 stress fractures, with only anecdotal descriptions published before 2010 [1, 2]. Since then, Hetsroni et al. [11] investigated whether a high arch was implicated, but they did not find static architectural differences in patients with stress fractures of the M5. In a 2013 study, Lee et al. [16] investigated factors for recurrent M5 fractures that had been surgically treated with tension band wiring and grafting. They found that increased weight, increased fourth to fifth intermetatarsal axial angle, and inclination angle were associated with higher ORs of refractures, but all refractures had a postunion history of subsequent trauma, so their conclusions may not be applicable to true stress fractures. We deem that inconsistencies in previous reports may arise from the older standard of imaging; the conventional sequence of 2D radiographs followed by multidetector CT is unfit either for 3D evaluation of the anatomy or nonweightbearing, resulting in biased measurements. Therefore, the use of weightbearing CT in the present study makes our findings probably more reliable and clinically relevant.

Assessing the specific M5 orientation parameters required time-consuming manual measurements or the use of advanced software, which may not be practical to apply in a clinical workflow. Hence, we assessed simple

weightbearing CT visual signs based on semiautomatic measurements, which are faster and more convenient, that were strongly associated with stress fractures: an M5 base touching the ground plane before the head, an M5 base closer than 10 mm to the ground plane, and a center of the ankle projecting outside (lateral) of the FAO tripod. Such assessments could be part of the clinical workflow and help screen patients at high risk. Of note, measurement of the FAO considering the lowest point on the M5 head as originally described could be thought of differently when the base is closer to the ground. Indeed, mechanical balance of the foot and ankle complex dictates that the tripod and the ankle should be superimposed. Precise offset measurements have been previously described, with the normal range at 2.3% ± 2.9% [20]. Considering this, our results show that the M5's location closer to the ground plane can be seen not only as disorder, but also as an adaptative mechanism akin to a kickstand mechanism that results in widening the foot tripod in an attempt to bring it back under the ankle when the ankle projects outside of the borders of the tripod (Fig. 12). Indeed, while the FAO was different in the stress fractures group and controls, this was not the case with the modified FAO. The sequences of results therefore seem to indicate that hindfoot varus may be a driver of M5 inclination, resulting in approximation between it and the ground plane, accompanied with fat pad compression (or possibly atrophy) under its base, as the center of the ankle projects over and beyond the lateral foot border. This is where a simple visual tool such as the FAO tripod can conveniently monitor the 3D relationship of the talus point with the foot tripod. A simple interpretation could therefore be that as long as the talus point remains within the tripod, the foot remains balanced. The more the talus point projects toward the lateral foot border, the lower and denser the M5 base presents to provide more stability and density as an adaptative mechanism to having the same weight projected on a smaller surface area. This interpretation remains speculative at this stage and warrants validation through larger studies.

We found a relative HU M5/HU talus density ratio increase of close to 50% on average compared with controls with a cutoff value at 20%. In the past, authors also report that athletes with bone stress fractures present with impaired cortical bone microarchitecture and decreased bone mineral density [31], while others mention decreased bone marrow density and vitamin D deficiency [23] as risk factors. As stress fractures result from initial microstructural changes that can typically only be identified through a bone scan or MRI (usually not prescribed initially), and as they often present with delayed onset and diagnoses, timely use of preventive measures where relevant is often not possible. We deem that our calculated ratio could be useful in accelerating this pathway and providing data to support and monitor preventive measures. Calcium supplementation, specific calf and intrinsic physical training, stretches, and custom orthotics have been reported [35]. However, little evidence is available as to their potential benefits. Other preventive measures could be considered such as change of shoe wear and modification or reduction of activity levels.

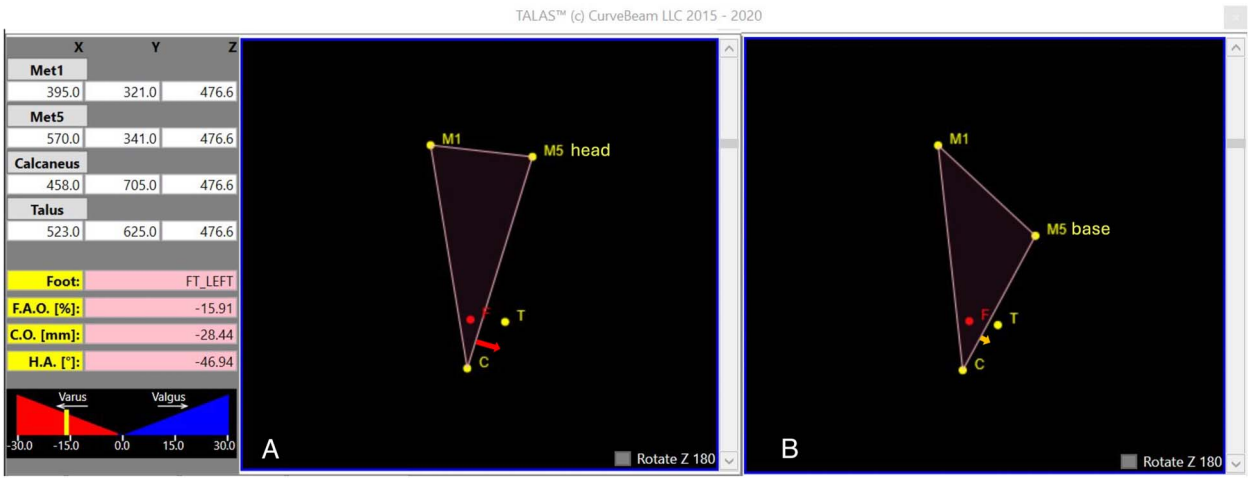

Fig. 12 The FAO measures the torque from the ankle's position relative to the foot tripod. (**A**) The FAO uses the M5 head as the ground contact point. The red arrow illustrates the offset between the talus point and the lateral border of the foot. (**B**) The FAO uses the M5 base instead of the head to account for anatomic changes. This adjustment enlarges the foot tripod, aligning it under the ankle's center talus (T) point, reducing deforming stresses on the hindfoot, similar to a motorcycle's kickstand preventing toppling. The yellow arrow illustrates the modified offset between the T point and the lateral border of the foot. F = foot center defined by intersection of the foot bisector and its perpendicular passing through T; C = calcaneus weightbearing point. A color image accompanies the online version of this article.

Conclusion

For this weightbearing CT study of a small patient cohort, increased bone density by > 20% above talus value was highly specific of being part of the stress fractures group. Simple visual assessment of M5 height, declination, and the projection of the center of the ankle relative to the FAO tripod could help identify patients at risk of M5 stress fractures. We also confirmed hindfoot varus and metatarsus adducts as associated factors. The findings of the present pilot work may also apply to other stress fractures in the foot and ankle, provided that specific studies are carried out. Ultimately, this method could serve in clinical settings to detect patients at risk of a stress fracture. Prospective studies should be carried out using weightbearing CT as a screening tool to compare those specific alignment and density parameters in patients who present a stress fracture down the line versus those who do not. This may help to determine more precise thresholds backed by larger cohorts.

Acknowledgment We thank Kevin Dibbern PhD for his mentoring and help with the 3D Slicer software.

References

1. Anderson EG. Fatigue fractures of the foot. *Injury*. 1990;21: 275-279.
2. Arangio GA, Xiao D, Salathe EP. Biomechanical study of stress in the fifth metatarsal. *Clin Biomech (Bristol, Avon)*. 1997;12: 160-164.
3. Bernasconi A, Cooper L, Lyle S, et al. Pes cavovarus in Charcot-Marie-Tooth compared to the idiopathic cavovarus foot: a preliminary weightbearing CT analysis. *Foot Ankle Surg*. 2021;27: 186-195.
4. Boden BP, Osbahr DC. High-risk stress fractures: evaluation and treatment. *J Am Acad Orthop Surg*. 2000;8:344-353.
5. Borjali A, Ashkani-Esfahani S, Bhimani R, et al. The use of deep learning enables high diagnostic accuracy in detecting syndesmotic instability on weight-bearing CT scanning. *Knee Surg Sports Traumatol Arthrosc*. 2023;31:6039-6045.
6. Brockwell J, Yeung Y, Griffith JF. Stress fractures of the foot and ankle. *Sports Med Arthrosc Rev*. 2009;17:149-159.
7. de Cesar Netto C, Myerson MS, Day J, et al. Consensus for the use of weightbearing CT in the assessment of progressive collapsing foot deformity. *Foot Ankle Int*. 2020;41:1277-1282.
8. de Cesar Netto C, Schon LC, Thawait GK, et al. Flexible adult acquired flatfoot deformity: comparison between weight-bearing and non-weight-bearing measurements using cone-beam computed tomography. *J Bone Joint Surg Am*. 2017;99: e98.
9. Gefen A. Biomechanical analysis of fatigue-related foot injury mechanisms in athletes and recruits during intensive marching. *Med Biol Eng Comput*. 2002;40:302-310.
10. Heaslet MW, Kanda-Mehtani SL. Return-to-activity levels in 96 athletes with stress fractures of the foot, ankle, and leg: a retrospective analysis. *J Am Podiatr Med Assoc*. 2007;97:81-84.
11. Hetsroni I, Nyska M, Ben-Sira D, et al. Analysis of foot structure in athletes sustaining proximal fifth metatarsal stress fracture. *Foot Ankle Int.* 2010;31:203-211.
12. Hughes LY. Biomechanical analysis of the foot and ankle for predisposition to developing stress fractures. *J Orthop Sports Phys Ther*. 1985;7:96-101.
13. Jones R. I. Fracture of the base of the fifth metatarsal bone by indirect violence. *Ann Surg*. 1902;35:697-700.2.
14. Korpelainen R, Orava S, Karpakka J, Siira P, Hulkko A. Risk factors for recurrent stress fractures in athletes. *Am J Sports Med*. 2001;29:304-310.
15. Lawrence SJ, Botte MJ. Jones' fractures and related fractures of the proximal fifth metatarsal. *Foot Ankle*. 1993;14:358-365.
16. Lee K, Park Y, Jegal H, Kim K, Young K, Kim J. Factors associated with recurrent fifth metatarsal stress fracture. *Foot Ankle Int*. 2013;34:1645-1653.
17. Lintz F, Bernasconi A, Baschet L, et al. Relationship between chronic lateral ankle instability and hindfoot varus using weight-bearing cone beam computed tomography. *Foot Ankle Int*. 2019; 40:1175-1181.
18. Lintz F, Bernasconi A, Buedts K, Welck M, Ellis S, de Cesar Netto C. Ankle joint bone density distribution correlates with overall 3-dimensional foot and ankle alignment. *J Bone Joint Surg Am*. 2023;105:1801-1811.
19. Lintz F, Mast J, Bernasconi A, et al. 3D, weightbearing topographical study of periprosthetic cysts and alignment in total ankle replacement. *Foot Ankle Int*. 2020;41:1-9.
20. Lintz F, Welck M, Bernasconi A, et al. 3D biometrics for hindfoot alignment using weightbearing CT. *Foot Ankle Int*. 2017;38: 684-689.
21. Mandell JC, Khurana B, Smith SE. Stress fractures of the foot and ankle, part 1: biomechanics of bone and principles of imaging and treatment. *Skeletal Radiol*. 2017;46:1021-1029.
22. O'Malley MJ, Hamilton WG, Munyak J, DeFranco MJ. Stress fractures at the base of the second metatarsal in ballet dancers. *Foot Ankle Int*. 1996;17:89-94.
23. Paavana T, Rammohan R, Hariharan K. Stress fractures of the foot - current evidence on management. *J Clin Orthop Trauma*. 2024;50:102381.
24. Payo-Ollero J, Álvarez Goenaga F, Elorriaga Sagarduy G, Ruiz Nasarre A, Olmos-García MA, Villas Tomé C. Stress fracture of the fifth metatarsal in foot deformity secondary to neuromuscular disease: experiences of deformity correction treatment-a report of 3 cases and review of the literature. *Foot Ankle Spec*. 2018;11: 177-182.
25. Ranjit S, Sangoi D, Cullen N, Patel S, Welck M, Malhotra K. Assessing the coronal plane deformity in Charcot Marie tooth cavovarus feet using automated 3D measurements. *Foot Ankle Surg*. 2023;29:511-517.
26. Richter M, Seidl B, Zech S, Hahn S. PedCAT for 3D-imaging in standing position allows for more accurate bone position (angle) measurement than radiographs or CT. *Foot Ankle Surg*. 2014;20: 201-207.
27. Richter M, Zech S, Naef I, Duerr F, Schilke R. Automatic software-based 3D-angular measurement for weight-bearing CT (WBCT) is valid. *Foot Ankle Surg*. 2024:S1268-7731(24) 00041-9.
28. Rizzone KH, Ackerman KE, Roos KG, Dompier TP, Kerr ZY. The epidemiology of stress fractures in collegiate student-athletes, 2004-2005 through 2013-2014 academic years. *J Athl Train*. 2017;52:966-975.
29. Sandlin MI, Rosenbaum AJ, Taghavi CE, Charlton TP, O'Malley MJ. High-risk stress fractures in elite athletes. *Instr Course Lect*. 2017;66:281-292.
30. Smith JW, Arnoczky SP, Hersh A. The intraosseous blood supply of the fifth metatarsal: implications for proximal fracture healing. *Foot Ankle*. 1992;13:143-152.

31. Stürznickel J, Hinz N, Delsmann MM, Hoenig T, Rolvien T. Impaired bone microarchitecture at distal radial and tibial reference locations is not related to injury site in athletes with bone stress injury. *Am J Sports Med*. 2022;50:3381-3389.
32. Sun J, Feng C, Liu Y, et al. Risk factors of metatarsal stress fracture associated with repetitive sports activities: a systematic review. *Front Bioeng Biotechnol*. 2024;12:1435807.
33. Theodorou DJ, Theodorou SJ, Boutin RD, et al. Stress fractures of the lateral metatarsal bones in metatarsus adductus foot deformity: a previously unrecognized association. *Skeletal Radiol*. 1999;28:679-684.
34. Torg JS, Balduini FC, Zelko RR, Pavlov H, Peff TC, Das M. Fractures of the base of the fifth metatarsal distal to the tuberosity: classification and guidelines for non-surgical and surgical management. *J Bone Joint Surg Am*. 1984;66:209-214.
35. Warden SJ, Davis IS, Fredericson M. Management and prevention of bone stress injuries in long-distance runners. *J Orthop Sports Phys Ther*. 2014;44:749-765.
36. Zaidi R, Sangoi D, Cullen N, Patel S, Welck M, Malhotra K. Semi-automated 3-dimensional analysis of the normal foot and ankle using weight bearing CT: a report of normal values and bony relationships. *Foot Ankle Surg*. 2023;29:111-117.
37. Zhang JZ, Lintz F, Bernasconi A, Weight Bearing CT International Study Group, Zhang S. 3D biometrics for hindfoot alignment using weightbearing computed tomography. *Foot Ankle Int.* 2019;40:720-726.